International Journal of Modern Physics A
Vol. 20, Nos. 20 & 21 (2005) 5037–5058

J/Ψ PRODUCTION IN HIGH ENERGY PARTICLE AND NUCLEAR COLLISIONS: SUPPRESSED, ENHANCED, OR JUST NORMAL?

P. GUPTAROY

Department of Physics, Raghunathpur College,
P.O. Raghunathpur 723133 Dist., Purulia (WB), India
gpradeepta@hotmail.com

GOURI SANYAL

Department of Physics, Lady Brabourne College, Kolkata-700017, India

BHASKAR DE

Institute of Mathematical Sciences,
C.I.T. Campus, Taramani, Chennai-600113, India
bhaskar@imsc.res.in

S. BHATTACHARYYA*

Physics and Applied Mathematics Unit (PAMU),
Indian Statistical Institute, Kolkata-700108, India
bsubrata@www.isical.ac.in

Received 8 September 2004

The oncoming recent data on production of J/Ψ mesons in some high energy particle and nuclear collisions are of special importance in view of the controversies centering around the so-called suppression or enhancement mechanisms for this particle-species. We will try to explain here the features of some of the basic observables on J/Ψ production with the help of an approach which has no direct links with quark–gluon plasma (QGP) considerations, but can interpret a large amount of data related to the proposed physical signatures of QGP. The final outcome, based on the present study, amounts to stating the fact that the J/Ψ production is neither suppressed nor enhanced; rather it exhibits both in our theoretical approach and also in the experimental measurements a behavior which is just as normal as many other secondaries, with only specificities of its own intrinsic quantum numbers and the very massive nature.

Keywords: Relativistic heavy ion collisions; inclusive production; quark–gluon plasma.

PACS numbers: 25.75.-q, 13.85.Ni, 12.38.Mh

*Corresponding author.

1. Introduction

The field of J/Ψ meson production is believed to be of special importance for two reasons: (a) the total and differential cross-section for J/Ψ production might provide valuable tests of what is viewed as quark–gluon plasma (QGP) state as well as some wealth of information on hadron structure functions; (b) besides, the studies on J/Ψ mesons are expected to reveal the nature of evolution of the "QGP" itself in vacuum. The main problem with the hypothesis of QGP lies in the fact that it cannot be detected directly,[1] for which there are only speculations about some indirect signatures.[2,3] One of the very important proposed signatures is the prediction on the "suppression" of J/Ψ-meson production in the nuclear collision, at certain stages; and also a prediction on an anomalous "enhancement" at certain other stage[4] as well. But qualitative predictions on such two-tier behaviors of J/Ψ mesons are based entirely on some phenomenological considerations which suffer from a high degree of arbitrariness. In the quantitative plane, the constraints on the physical behavior spring up from a physical factor arising out of the QCD-inspired approaches.[4] The deciding factor, in terms of the Standard Model (SM), is the number of charm–anticharm ($c\bar{c}$) pairs ($N_{c\bar{c}}$) created in the early stage of hard parton collisions in $A + A$ (or in $A + B$) reactions. On the basis of it, Gorenstein *et al.*[4] arrived at the predictions of the J/Ψ suppression (at $N_{c\bar{c}} < 1$) and the J/Ψ enhancement (at $N_{c\bar{c}} > 1$) effects. But in our study we do not lay much importance to all such predictive observations, as we would like to proceed somewhat independently without any specific bias and prejudice. However, the experimental measurements on the real physical observables in various high energy hadronic and nuclear collisions constitute here our prime concern. The main points of interest rest on the following facts: (i) the issue is still much topical, and is somewhat controversial.[5–10] (ii) And this is an exciting issue because of the fact that the behavior of the production of Ψ-mesons in both particle and nuclear collisions at high energies is not yet properly understood. Besides, the issue has also a fair degree of theoretical importance as is outlined below.

The proposal for "suppression" of J/Ψ mesons as the signal for QGP formation is grounded on the argument that at sufficiently high temperatures the QGP screens the heavy quark potential, thus preventing formation of any bound state producing Ψ mesons which is assumed to be composed of $c\bar{c}$. This was given a two-sector tilt by Gorenstein *et al.*[4] as indicated here earlier.

Our objective here, is to interpret a substantial part of the significant J/Ψ production data measured by different groups[11–24] at different energies with the help of a model which has no direct QGP tag and with some ancillary physical ideas. But the task would be a difficult one, as the terrain is embedded with problems. First, the manifestation in the data of final state "suppression" is still not beyond doubt. Although the signature is proposed, it is not easy to identify a concrete observable for calculation on the proposed behaviors for experimental verification. There are many theoretical and experimental uncertainties which make the claim for existence

of QGP very difficult even with the proposed signatures.[25–30] So, one should refrain from arriving at any hasty conclusions — either in favor or in opposition to — the possible "evidences" for QGP formation. Second, the measured suppression, if any, is only a relative one, with respect to a continuum which is not fully understood. There are many ambiguities in the data recoding and measurements.

The paper is organized as follows: in Sec. 2 we present a synopsis and outline of the controversy on suppression versus enhancement. Subsection 3.1 deals with the model that we would like to apply in our work here. In Subsec. 3.2 we try to provide an extension of the said model for the multiple production of J/Ψ particles in ep collisions. In Sec. 4 we focus on the results obtained and their model-based interpretations. Lastly, Sec. 5 contains the concluding remarks.

2. Suppression, Increased Suppression versus Enhancement: A Synopsis of the Controversy

The controversy has arisen out of no clear and decisive observations made so far either in favour of or against the model-based predictions. From the very outset, the controversy springs merely from the projections made by various versions of the SM phenomenology. A modest degree of suppression of J/Ψ particles was anticipated from what is known as screening of the so-called $c\bar{c}$ (charm–anticharm) pair formations. The excess "suppression" reported by NA50 collaboration[31–34] in Pb + Pb collisions appeared to be a great puzzle. Once again, this so-called anomaly was reflected by the degree of suppression that exceeds the one expected from the model-based extrapolation of the $P + A$ and $S + A$ data. This additional suppression was attempted to be explained by various phenomenological factors: (i) the Comovers Approach (CoM),[32–34] (ii) Gluon-depletion (GD) approach.[35] These two approaches would be sketched hereafter. But, prior to taking this up, let us stress on the piece of information that there is a phenomenological model which reveals no suppression, rather predicts at the highest RHIC energy, J/Ψ "enhancements."[4] And this intensifies the degree of controversy.

According to the comover approach[32–34] the production in nuclear collisions occurs in multiple stages and the secondaries are produced even though the interactions between the energetic particles after the initial (vigorous) collisions is over. According to this CoM model, the J/Ψ survival probability is thus, the product of two factors $S_{\rm abs}(b,s)$. $S_{co}(b,s)$, where b is the impact parameter and s is the center-of-mass energy square. The first factor represents the so-called standard "suppression" due to nuclear absorption of the $c\bar{c}$ pair, *á la* the SM. The expression for it is given by the probabilistic Glauber model and is quite well known. Obviously, the model has a parameter introduced by $S_{\rm abs}$ and symbolized by the absorption cross-sections $\sigma_{\rm abs}$. The second term represents the excess suppression arising out of the interactions with comovers and this received some detailed phenomenological treatment within the confines of the dual parton model.[33] This led to the claim of explaining the data from NA50 collaboration[12–15] on properties of J/Ψ production from peripheral collisions up to the knee of transverse energy (E_T) distribution.

The second approach also does provide support to enhanced suppression to production of Ψ particles by the GD through the multiple secondary interactions after the initial highly energetic primary (hard) interaction is over. The GD approach[35] is really a bit unconventional, because it is not based on the usual assumption in the parton distributions in protons and are not affected by proton-propagation through the nucleus. This leads, finally and somewhat automatically, to the property of factorization which is found to be modestly valid for $PP/P\bar{P}$ or hadronic reactions at high energies but is not beyond question for the cases of nucleus-involved and purely nuclear collisions. The approach, thus, inducts modifications or distortions in the parton distribution functions by the nonperturbative processes and examines the effect on J/Ψ suppression. On the basis of this, Hwa *et al.*[35] justified J/Ψ suppression.

On the contrary, Gorenstein *et al.*[4] proposed some methods for formations of the open and hidden charm particles at late hadronization stage which are supposed to follow the prescription of statistical mechanics. According to this, J/Ψ mesons are created at the hadronization stage similar to other lighter hadrons. At this stage they are formed due to the coalescence (recombination) of charm (c) and anticharm ($\bar{c}$) which are produced by primary hard parton collisions at the initial stage. Gorenstein *et al.* used the canonical ensemble formulation of the statistical coalescence model. This led them to propound the idea of J/Ψ enhancement with the additional source of charmonium production. More particularly, an increase of the $\langle J/\Psi \rangle$ to $N_{c\bar{c}}$ ratio is expected. With the incorporation of this mechanism, Gorenstein *et al.* predicted J/Ψ enhancement at the highest RHIC energy collisions involving Au Au nuclei. But this is also the offshoot of some assumptions and thus is fully phenomenological.

But in our approach we deliberately cease to accept in an *a priori* manner any of these predictions or postulates. Rather, we want to give emphasis only on the real data-issues related to the problem, i.e. J/Ψ production, in question; and to give a fresh look to it with some radical views. Our singular objective here would be to explain the various sets of up-to-date data on production of J/Ψ particles in various high energy particle and nuclear collisions from the viewpoint of the effective and probable combinations of some models (EPCM's) of which the sequential chain model (SCM) for multiple production of secondary particles in PP interactions at high energies is an integral part. The other components arise out of the need to transform the results of NN (PP) reactions to those for NA or AB interactions at high energies. Depending on the studied observable(s) the route is, at times, quite straightforward and sometimes somewhat roundabout.

3. Outline of the Model

Here, in the first subsection, we deal with the production of the J/Ψ in nucleon–nucleon (NN) interactions. Thereafter, we present a very brief sketch of J/Ψ production mechanism for ep collisions, though we offer no separate diagrammatic

representation as the basic model for multiple production of J/Ψ particles remains the same as that for PP interaction at high energies. The relevant transitions for different observables from NN collisions to AB interactions will be discussed in the respective subsections.

3.1. *The specific J/Ψ production model in NN (PP) collisions: An approach*

We will use here a particular version of Sequential Chain Model (SCM)[36–42] to study some of the main characteristics and crucial observations related to production of π-mesons and J/Ψ mesons in different particle and nuclear collisions at high energies. Let us first recapitulate some of the salient features and important physical characteristics of the SCM valid for hadron–hadron and lepton–hadron collisions. According to this model, high energy hadronic interactions boil down, essentially, to the pion–pion interactions; as the protons are conceived in this model as $P = (\pi^+\pi^0\vartheta)$, where ϑ is a spectator particle needed for the dynamical generation of quantum numbers of the nucleons. The production of pions in the present scheme occurs as follows: the incident energetic π-mesons in the structure of the projectile proton (nucleon) emits a rho (ϱ)-meson in the interacting field of the pion lying in the structure of the target proton, the ϱ-meson then emits a π-meson and is changed into an omega (ω)-meson, the ω-meson then again emits a π-meson and is transformed once again into a ϱ-meson and thus the process of production of pion-secondaries continue in the sequential chain of ϱ-ω-π mesons. The two ends of the diagram contain the baryons exclusively. Figure 1 depicts the mechanisms for production of pions of all three varieties in PP collision.

The production of J/Ψ in proton–proton and pion–proton collisions is similar to that of pion production in this model. The π-meson emits a ϱ-meson, the ϱ-meson then emits a π-meson and is changed into a ω-meson, the ω-meson emits a photon, then the photon emits a J/Ψ particle. From the viewpoint of the present model, the

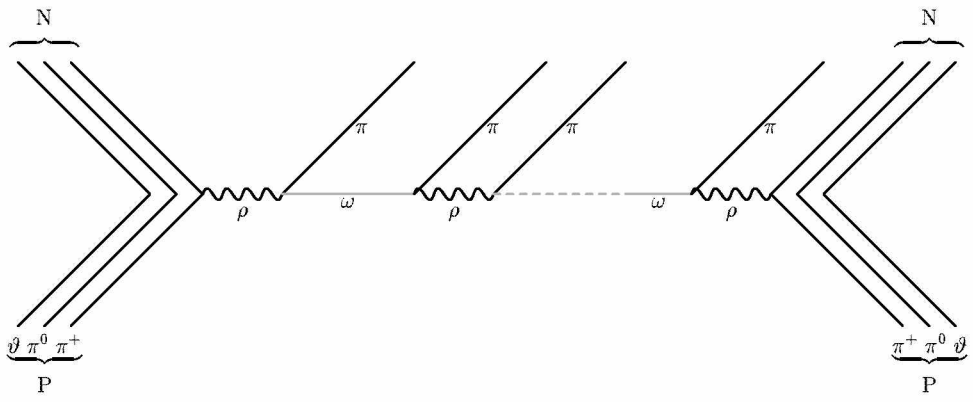

Fig. 1. Schematic diagram of multiple production of pions in PP scattering in the present scheme.

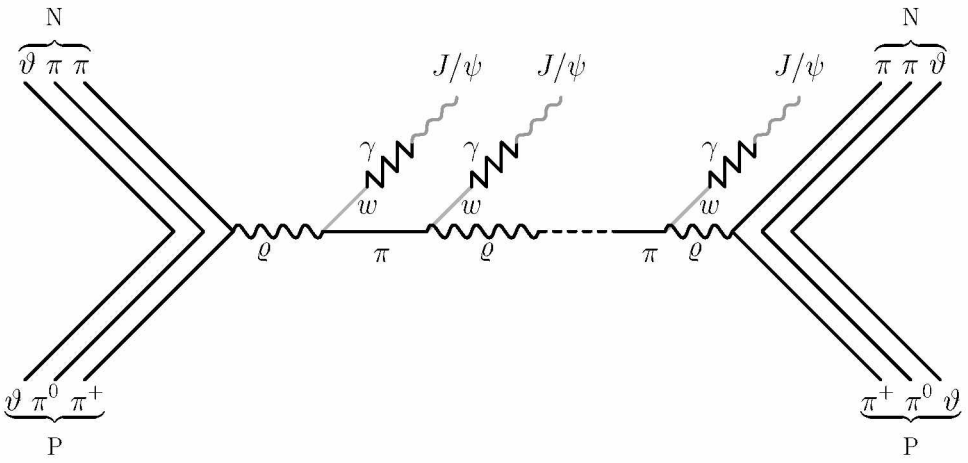

Fig. 2. Schematic diagram of multiple production of J/Ψ particles in PP scattering in the present scheme.

π-meson is transformed once again into ϱ-meson and the process of J/Ψ production continues. Figure 2 depicts the mechanisms for production of J/Ψ particles in PP collision.

Let us now proceed to present a summary of some of the useful results to be utilized here for the present work. The details of calculations are given in Refs. 36–42. It is to be noted that the assorted expressions given below are derived on the basis of rigorous field theoretic considerations for the inclusive production cross-sections and average multiplicity values of the J/Ψ particles and of various types of secondary pions (of any variety) produced in the sequential chain.[36–42]

The inclusive cross-section of the Ψ-meson produced in PP collisions given by

$$E\frac{d^3\sigma}{dp^3}\bigg|_{PP\to J/\Psi x} \cong C_{J/\Psi}\exp\left[\frac{-5.35(p_T^2+m_{J/\Psi}^2)}{\langle n_{J/\Psi}\rangle_{PP}^2(1-x)}\right]\exp(-1.923\langle n_{J/\Psi}\rangle_{pp}x)\,, \quad (1)$$

where the expression for average multiplicity of Ψ-particles in PP scattering would be given by

$$\langle n_\Psi\rangle_{PP} \approx 4\times 10^{-6}s^{1/4}\,. \quad (2)$$

In the above expression, the term $|C_{J/\Psi}|$ is a normalization parameter and is assumed here to have a value $\cong 0.09$ for Intersecting Storage Ring (ISR) region, and it is different for different region and for various collisions. The terms p_T, x and $m_{J/\Psi}$ represent the transverse momentum, Feynman scaling variable and the rest mass of the J/Ψ particle, respectively. Moreover, by definition, $x = 2p_L/\sqrt{s}$ where p_L is the longitudinal momentum of the particle. For all practical purposes, x-values for Ψ production are too small compared to unity for which $(1-x)$ factor in the denominator of the exponent form as treated as unity for all further calculations.

Similarly, the expression for inclusive cross-section for the neutral pions can be written in the following form:

$$E\frac{d^3\sigma}{dp^3}\bigg|_{PP\to\pi^0 x} \cong C_{\pi^0}\exp\left[\frac{-26.88p_T^2}{\langle n_{\pi^0}\rangle_{PP}(1-x)}\right]\exp(-2.38\langle n_{\pi^0}\rangle_{PP}x)\,, \tag{3}$$

where $|C_\pi| \simeq 90$ for ISR energy region and with the following relation for $\langle n_{\pi^0}\rangle$:

$$\langle n_{\pi^0}\rangle_{PP} \simeq \langle n_{\pi^-}\rangle_{PP} \simeq \langle n_{\pi^+}\rangle_{PP} \simeq 1.1s^{1/5}\,. \tag{4}$$

The expression for average transverse momentum for any secondary (c), by definition, is

$$\langle p_T\rangle^c = \frac{\int_{p_T(\min)}^{p_T(\max)} p_T\left(E\frac{d^3\sigma}{dp^3}\right)^C dp_T^2}{\int_{p_T(\min)}^{p_T(\max)}\left(E\frac{d^3\sigma}{dp^3}\right)^C dp_T^2}\,. \tag{5}$$

Using the above definition and putting the form of inclusive cross-section given by Eq. (15), into use we arrive at

$$\langle p_T\rangle_{pp}^{J/\Psi} \cong \kappa s^{3/16}\ \text{GeV}/c\,, \tag{6}$$

where κ is a constant and is taken here to be given by $\kappa \cong 0.15$ for ISR energy region.

3.2. *The model for ep collisions or e^+e^- annihilations*

The model for multiple production of J/Ψ particles in ep collisions or in e^+e^- annihilations would be somewhat exactly similar to that for PP collisions (Fig. 2) on the right-hand side; but there would be a difference only in the left-hand side vertex. In both these reactions (ep collisions or e^+e^- annihilations) the left-hand side will have to be replaced by $e^- \to e^-\gamma$, or $e^+e^- \to \gamma$; and these free and excited photons could release ρ^0-meson. Once stated, the $\rho^0-\omega-\pi$ chain could start working depending on the degree of excitation of the ρ^0-meson and on the rho-omega-pion coupling strength. The chain might continue to yield finally J/Ψ particles obviously as in PP interaction case. And after the continuity of the sequential chain up to a few successive stages which depends on the net available energy for hadronization, the right-hand side vertex ends up in exactly the same way, as the target is proton in ep collisions.

The mechanisms suggested here for ep reactions or for e^+e^- annihilations are fully consistent with the conservation rules and also with the canons of selection principles of particle physics. Despite the differences that are necessitated here for diagrammatic and physical representation of the emissions of J/Ψ particles, the final calculations are found to be virtually independent of them.

4. Model-Based Analyses and the Results

There are some data on diverse aspects of J/Ψ particles for various different sets of collisions. What we need to emphasize is that the observables are different for different collisions at the same or separate energies. So let us split up the cases and treat the data available on them, one by one, individually and on a case-to-case basis.

In this section, at first, we would like to discuss the rapidity and transverse momentum distribution of J/Ψ particles in $e-p$ collisions. In the next subsection, we will take up the average multiplicity ratio of J/Ψ particles to the negatively charged hadrons ($\langle J/\Psi\rangle/\langle h^-\rangle$) against the c.m. energy of the nucleonic system ($\sqrt{s}$) and also against the participant nucleons ($N_{\rm part}$) of the nucleus–nucleus collisions. Subsection 4.3 will provide average transverse momentum distributions of the particle for different proton and pion induced nuclear reactions. In Subsec. 4.4 we will deal with the production of J/Ψ particles in Oxygen–Uranium reaction at 200 GeV $\cdot$ A. In the next subsection, the transverse momentum distribution of J/Ψ particles in Pb – Pb collisions at 158 GeV $\cdot$ A will be taken into account. Lastly, we will make some predictions for some of the properties of J/Ψ particles in Au – Au collisions at Relativistic Heavy Ion Collider (RHIC).

4.1. *The rapidity and transverse momentum distribution in $e-p$ collisions $\sqrt{s}=300$ GeV*

For the calculation of rapidity distribution and the p_T^2 distribution from set of equations given above we can make use of two standard relations as given below:

$$\frac{d\sigma}{dy}=\int\left[E\frac{d^3\sigma}{dp^3}\right]d^2p_T\,, \tag{7}$$

$$\frac{d\sigma}{dp_T^2}=\int\left[E\frac{d^3\sigma}{dp^3}\right]dy\,. \tag{8}$$

The rapidity distribution and p_T^2 distribution for the inclusive J/Ψ production are calculated from Eqs. (1), (7) and (8) for the reaction of the type $e+p\rightarrow J/\Psi+x$ and are given by the following set of relations:

$$\frac{d\sigma}{dy}=696.56\exp(-0.12\sinh y_{cm})\,, \tag{9}$$

$$\frac{d\sigma}{dp_T^2}=75.76\exp(-0.14p_T^2)\,. \tag{10}$$

The solid lines in Figs. 3 and 4 show the theoretical SCM calculations while the data are taken from Ref. 22.

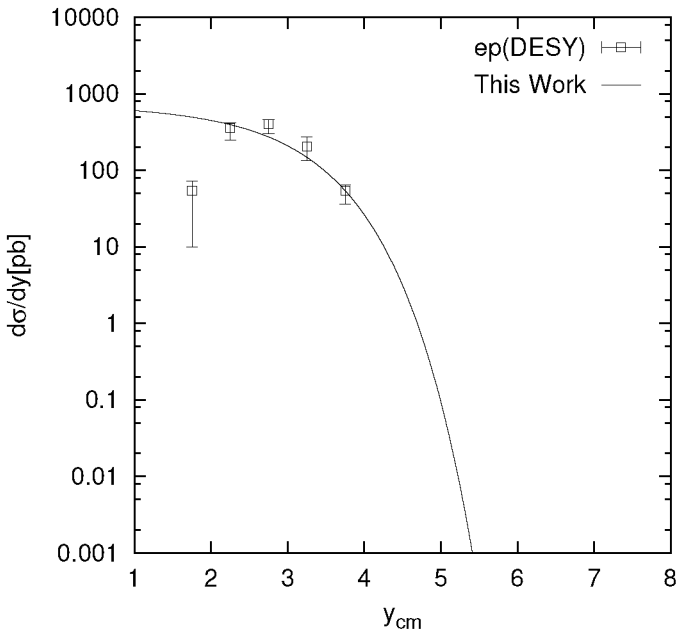

Fig. 3. Plot of the $y_{\rm cm}$ distribution of the J/Ψ inclusive production in ep collisions. Data points are from Ref. 22. Also shown are the theoretical SCM results by the solid curve.

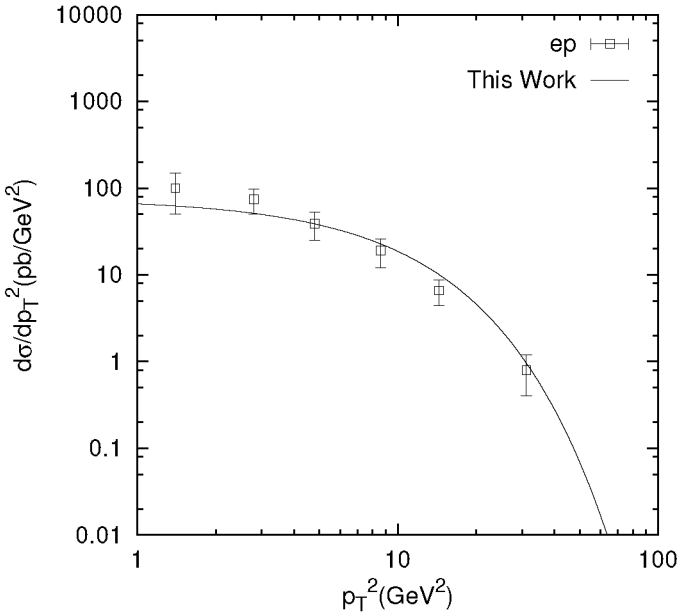

Fig. 4. Plot of the p_T^2 distribution of J/Ψ inclusive production in ep data taken from Ref. 22. The solid curve shows the theoretical SCM-based results.

4.2. *Characteristics of average multiplicity of the J/Ψ particles*

The study here is divided into two subsections: the first is for nucleon–nucleon (PP) reactions and the second is for nuclear reactions. Besides, in the first we will deal with the relationship between behavior and the c.m. energy, whereas in the next one, the link between average multiplicity ratio and the number of participants would be investigated.

4.2.1. *Average multiplicity ratio and c.m. energy in nucleon–nucleon reactions*

As pions constitute the main bulk of the negatively charged hadrons, we calculate the ratio, $R_{J/\Psi} = \langle n_{J/\Psi}\rangle_{PP}/\langle h^-\rangle_{PP}$, wherein $\langle n_{J/\Psi}\rangle_{PP}$ is the average multiplicity of the J/Ψ particles and $\langle h^-\rangle_{PP}$ is assumed to be given practically by the magnitude of the average multiplicity of negative pions. This is now done with the help of Eqs. (2) and (4) and is given by the following expression:

$$\frac{\langle n_{J/\Psi}\rangle_{PP}}{\langle h^-\rangle_{PP}} \times 10^6 = 0.7 s^{0.05}\,. \tag{11}$$

The data are taken from Ref. 28. The theoretical curve for the average multiplicity ratio versus the c.m. energy is plotted in Fig. 5 against the experimental background.

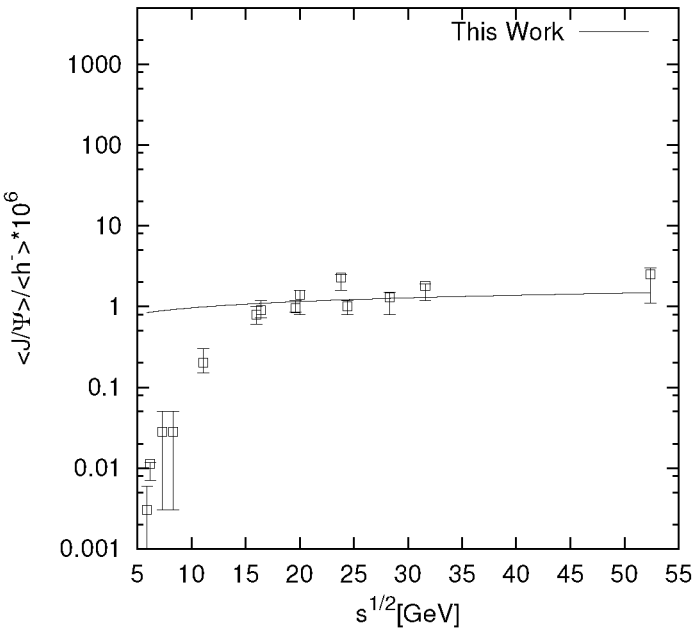

Fig. 5. The ratio of mean multiplicities of J/Ψ mesons and negatively charged hadrons for inelastic proton–nucleon interaction as a function of center-of-mass energy is plotted. Data sets are from Ref. 28. The line shows the theoretical SCM results.

4.2.2. *Average multiplicity ratio versus number of participants*

Our approach here would be based on an old assumption that inelastic nucleon–nucleus or nucleus–nucleus collisions at high energies could be described as incoherent superposition of the collisions of individual nucleons. Furthermore, in the light of the Glauber model (GM) it is also assumed that the contribution of the incident nucleon to the production of a particular species, denoted by the subscript "X," in a nucleon–nucleus (NA) collision is represented by $\langle n_X\rangle_{NA}$ and this would be same as the contribution of each hit target nucleon and this equals approximately to $\frac{1}{2}\langle n_X\rangle_{NN}$ with $\overline{W_A^N}(1) = 1$ for NA interactions. No reckoning of the factor of the number of times the nucleon suffers interaction is made. Accordingly, the extensions of the GM to nucleus–nucleus (AB) collisions is somewhat straightforward:[45]

$$\langle n_X\rangle_{AB} = \frac{1}{2}\left[\overline{W_A^N}(B) + \overline{W_B^N}(A)\right]\cdot\langle n_X\rangle_{NN}\,, \tag{12}$$

where $\overline{W_A^N}(B)$ indicates the average number of wounded nucleons of the target nucleus of mass number B in a collision with a projectile of mass number A.

For collisions between two nuclei of the same mass number, the above expression reduces to

$$\langle n_X\rangle_{AA} = \overline{W^N}(A)\langle n_X\rangle_{PP}\,. \tag{13}$$

Furthermore, Kadija *et al.*[45] also showed

$$\frac{\langle n_X\rangle_{AB}}{\langle n_{h^-}\rangle_{AB}} = \frac{\langle n_X\rangle_{NN}}{\langle n_{h^-}\rangle_{NN}}(F_{AB})^{-1}\,, \tag{14}$$

with

$$F_{AB} = \frac{\left[\overline{W_A^N}(B) + \overline{W_B^N}(A)\right]}{2W_A^X(B)}\,, \tag{15}$$

where F_{AB} is a scale factor related to the ratio values of the average wounded nucleons in AB collisions and the number of average wounded partons lying inside the protons contained in the nuclei. The factor F_{AB} is an indicator to the difference in the production mechanism of any species X and that for h^- production.

In a previous work[46] by one of the authors (SB here), the number of wounded nucleons in hadronuclear collisions ($\overline{W^N}$) was taken to be proportional to $N_p^{0.20}$ where N_p is the number of participant/wounded nucleons. But for AB or AA reactions we use here $\overline{W^N} \propto N_p^{0.22}$. And from the 5-parton model which is the basis of the SCM[36–42] for PP (NN) interaction here, we have taken $W_p^X \sim N_p^{0.20}$.

Now let us take the measured particle to be $\Psi(\equiv X)$ and treat NN reaction to be equivalent to PP reactions. Combining then, Eqs. (11), (14) and (15), and accommodating the points mentioned in the above paragraph we get the ratio value to be given by

$$\frac{\langle n_\Psi\rangle_{AB}\times 10^6}{\langle n_{h^-}\rangle_{AB}} = \frac{\langle n_\Psi\rangle_{NN}\times 10^6}{\langle n_{h^-}\rangle_{NN}}N_p^{-0.02} \sim 0.7s^{0.05}N_p^{-0.02}\,. \tag{16}$$

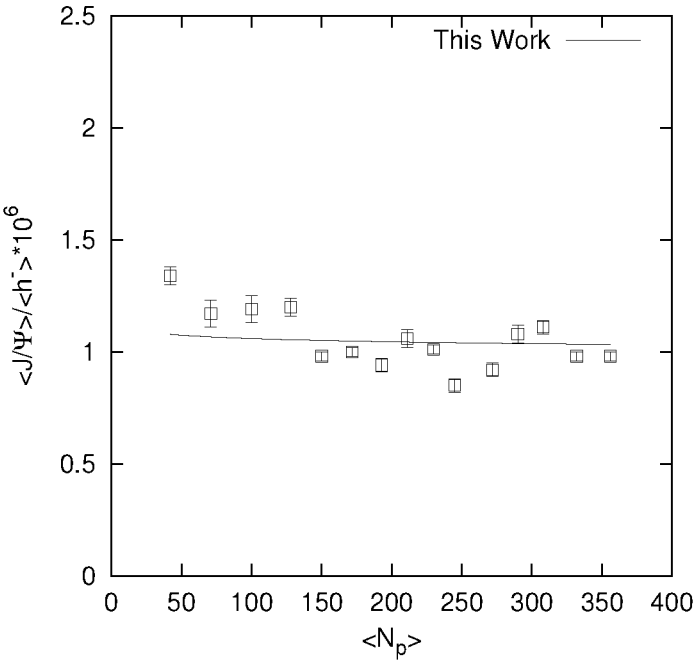

Fig. 6. The ratio of mean multiplicities of J/ψ mesons and negatively charged hadrons for inelastic O + Cu, O + U, S + U and Pb + Pb interactions at 158 GeV·A plotted as a function of number of participant nucleons. The results for Pb + Pb interactions measured for different centralities of collisions. Data are taken from Ref. 28. The line shows the theoretical SCM-based theoretical values.

In Fig. 6 we depict graphically the plot of Eq. (16) in a solid line against the data sets obtained from Gazdzicki and Gorenstein.[28] The expression gives a fair description of the data. It is to be noted that the expression (16) represents the resultant effect of the SCM-model and the elements of nuclear dynamics based on Glauberian concepts.

4.3. *Hadronuclear collisions and the average transverse momentum of J/Ψ*

Using Eq. (6) and fitting κ of that equation to 0.32 we obtain the expression for average transverse momentum of J/Ψ particle in the proton-induced nuclear reaction at various energies. This is given by the relation

$$\langle p_T \rangle_{pA}^{J/\Psi} \cong 0.32 s^{3/16} \text{ GeV}/c\,, \tag{17}$$

where A represents the target nucleus. For the present study the target nuclei are proton, carbon and beryllium. Figure 7 depicts the theoretical plot of $\langle p_T \rangle$ versus $s^{1/2}$ against the experimental results taken from different groups.[11,17–19]

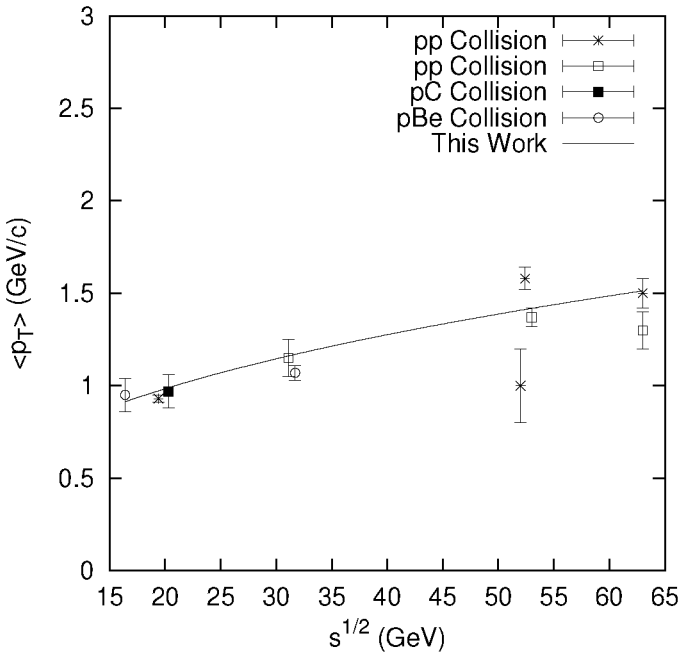

Fig. 7. Plot of the dependence of $\langle p_T \rangle$ on $\sqrt{s}$ for proton induced reactions. Data points are from Refs. 11, 17–19. The curve shows the theoretical SCM results.

Similarly, for the case of pion-induced reactions the value of κ would be fitted to 0.33 and the relation between $\langle p_T \rangle$ and s would be

$$\langle p_T \rangle_{\pi A}^{J/\Psi} \cong 0.33 s^{3/16} \text{ GeV}/c\,. \tag{18}$$

Here, A stands for p, C, Be, Cu and W particles. In Fig. 8 the line shows the theoretical plot of SCM-based equation against the experimental results.[11,19–21]

4.4. *Invariant p_T spectra in oxygen–uranium collisions at* **200 GeV·A**

To calculate dN/dp_T from $E(d^3\sigma/dp^3)$, we can make use of the following standard relation

$$\left.\frac{dN}{dp_T}\right|_{PP} = \frac{2p_T}{\sigma_{\text{in}}} \int \left.\frac{d^3\sigma}{dp_T^2 dy}\right|_{PP} dy\,, \tag{19}$$

where σ_{in} is the inelastic nucleon–nucleon cross-section.

With a view to studying the nature of different p_T-spectra for production of particles in any nucleus (A)–nucleus (B) collisions, we will have to build up a suitable connector between nucleon–nucleon and nucleus–nucleus interactions at high energies. In studying the differential p_T-spectra of hadrons in nuclear collisions let us assume first that the nature of relationship would be of similar type as that

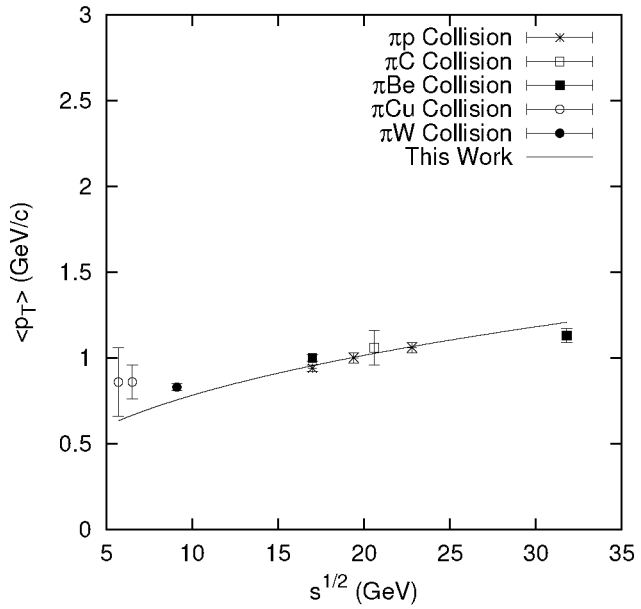

Fig. 8. Plot of the dependence of $\langle p_T \rangle$ on $\sqrt{s}$ for pion induced reactions. Data points are from Refs. 11, 19–21. The solid curve shows the theoretical SCM results.

between rapidity density of nuclear collisions with rapidity density in nucleon–nucleon (PP) reaction,[43] i.e.

$$\left.\frac{dN}{dp_T}\right|_{AB}[b] \approx \Delta \left.\frac{dN}{dp_T}\right|_{PP}, \tag{20}$$

where Δ contains some physical factors involving the nuclear dynamics and these are to be obtained from Wong.[43]

Let us assume that in a nucleus–nucleus (AB) collisions, each collision contributes to the production of particles, but the contributions from all of the collisions are not the same, because of the attenuation of the baryonic (protonic) energy while passing through the target nucleus. Let $n'(b)$ represents the number of inelastic nucleon–nucleon collisions at an impact parameter b. Had the contributions been uniform in all the collisions, the p_T-distribution, dN/dp_T for nucleus–nucleus collisions would just be $n'(b)$ times the p_T-distribution, $\left.\frac{dN}{dp_T}\right|_{PP}$ for nucleon–nucleon collisions. But this is not the case in reality because of the baryon-stopping by energy-attenuation. The effect of energy degradation should lead to a diminutive term of the form $\frac{1}{1+a'(A^{1/3}+B^{1/3})}$, when one uses a reduction factor to the first power in the thickness of the projectile and of the target nucleus. For the present calculations, we now use this reduction factor to represent the kernel of physics in building up the fly-over between the two-sets of p_T-differential spectra:

$$\left.\frac{dN}{dp_T}\right|_{AB} \simeq \frac{n'(b)}{1+a'(A^{1/3}+B^{1/3})} \left.\frac{dN}{dp_T}\right|_{PP}, \tag{21}$$

where a' is a parameter ($\ll 1$) to be chosen for any set of nucleus–nucleus interaction. For the present work the chosen values of a' is ~ 0.09.[43]

The estimation of $n'(b)$ is dependent upon the thickness functions and the use of the various forms of nuclear density distributions. On the basis of Woods–Saxon type of nuclear density distribution it was shown by Bialas *et al.*[44] that the number of inelastic nucleon–nucleon collisions, denoted by $n'(b)$, in any AB collisions is given by

$$n'(b) \simeq \frac{(A\sigma_B + B\sigma_A)}{\sigma_{AB}}\,, \tag{22}$$

where σ_A is the nucleon (proton)–nucleus (A) production cross-section, σ_B is the inelastic nucleon (proton)–nucleus (B) production cross-section and σ_{AB} is the inelastic production cross-section for the collision of nucleus A and nucleus B.

Finally, combining Eqs. (21) and (22), one arrives at

$$\left.\frac{dN}{dp_T}\right|_{AB} \simeq \frac{(A\sigma_B + B\sigma_A)}{\sigma_{AB}} \frac{1}{1 + a'(A^{1/3} + B^{1/3})} \left.\frac{dN}{dp_T}\right|_{PP}. \tag{23}$$

It is well known that the transverse energy, E_T, is usually written as[47]

$$E_T = \frac{1}{4}\,\pi E_i\,, \tag{24}$$

where

$$E_i = \sqrt{s} - m(N_p + N_t)\,, \tag{25}$$

corresponding to energy observed in a total absorption calorimeter. Here, m in the expression (25) is the nucleon mass, N_p and N_t are the number of projectile and participating target nucleons. This E_T-variable is introduced as the p_T-spectra have some dependence on it in the final forms of expressions as shown below.

By combining Eqs. (1), (19), (20) and (23)–(25), we obtain

$$\left.\frac{1}{p_T}\,\frac{dN}{dp_T}\right|_{OU} = 657.34\exp(-0.70p_T^2)\,, \quad \text{(Low } E_T\text{)} \tag{26}$$

and

$$\left.\frac{1}{p_T}\,\frac{dN}{dp_T}\right|_{OU} = 611.28\exp(-0.65p_T^2) \quad \text{(High } E_T\text{)}\,. \tag{27}$$

The experimental results are taken from NA38 group[23] and they are plotted in Figs. 9 and 10 for low and high E_T's. The model-based theoretical curves for J/Ψ are shown by the solid curves in those figures (Figs. 9 and 10).

4.5. *Nature of* $\langle p_T \rangle$ *versus* E_T *in* Pb + Pb *collision at* 158 GeV·A

The transverse energy distribution observed in the final state also provides some information about the initial state created and the abundant particle production.

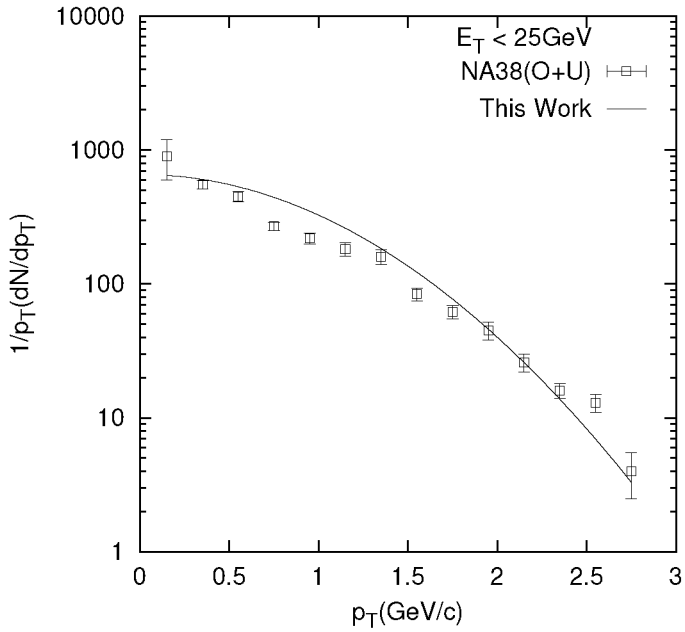

Fig. 9. Plot of the p_T distribution of J/Ψ for O – U interaction at 200 GeV·A for $E_T < 25$ GeV. Data are taken from Ref. 23. The solid curve presents the combinational results based on SCM.

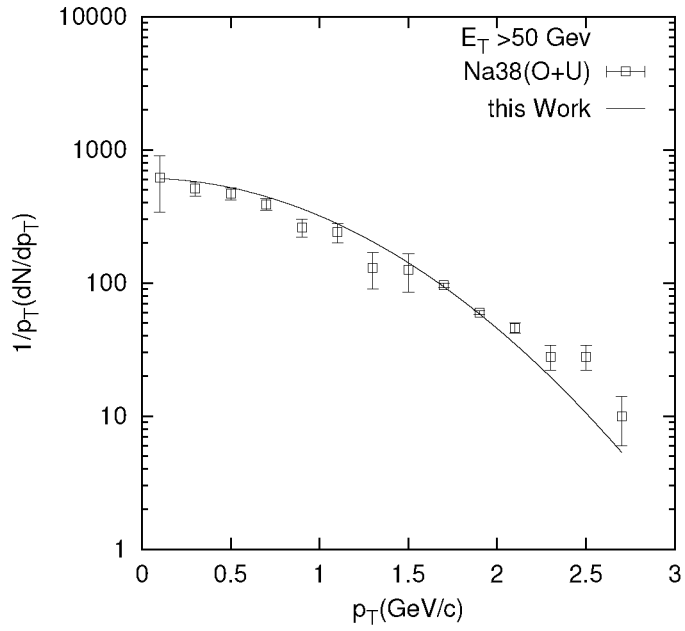

Fig. 10. Plot of the p_T distribution of J/Ψ for O – U interaction at 200 GeV·A for $E_T > 50$ GeV. Data are taken from Ref. 23. The solid curve represent in the SCM-based results.

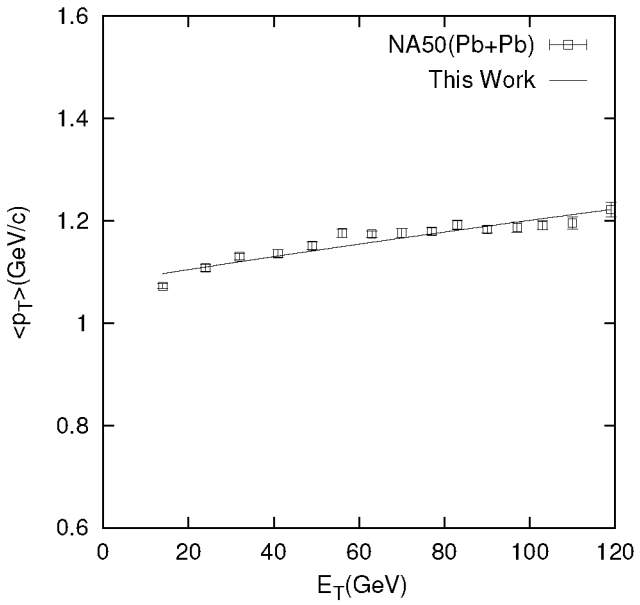

Fig. 11. Plot of the $\langle p_T \rangle$ as a function of the transverse energy for Pb+Pb collisions at 158 GeV·A. Data sets are taken from Ref. 12. The solid line depicts the SCM-based results.

Now, in finding out a relationship between the average transverse momentum $\langle p_T \rangle$ and the transverse energy E_T, we use Eqs. (6), (24) and (25). Finally, we arrive at the expression for transverse momentum of the produced J/Ψ particles in terms of E_T in $\mathrm{Pb}-\mathrm{Pb}$ collisions

$$\langle p_T \rangle_{\mathrm{Pb}+\mathrm{Pb}} \simeq 0.112(1.27E_T + 387.3)^{0.38} . \tag{28}$$

The experimental results are taken from NA50 group[12] and they are plotted in Fig. 11. The model-based theoretical curve for J/Ψ is shown by the solid curve in the same figure.

4.6. *Results and prediction for the RHIC experiments*: $\mathbf{Au-Au}$ *collisions at* $\sqrt{s} = 130$ **GeV** *and* **200 GeV**

In this subsection, we would like to analyze some recent results and to predict about the possible status of J/Ψ production in $\mathrm{Au}+\mathrm{Au}$ collisions at RHIC at $\sqrt{s} = 130$ GeV and 200 GeV with regard to some separate observables and they are being treated below in different subsections.

4.6.1. *Total* J/Ψ *cross-sections in PP collisions*

The total cross-section for J/Ψ production in PP collisions is calculated from Eq. (1). The relation for total cross-section in terms of c.m. energy now becomes

$$\sigma_{pp\to J/\Psi X} = 7.45 s^{0.72} . \tag{29}$$

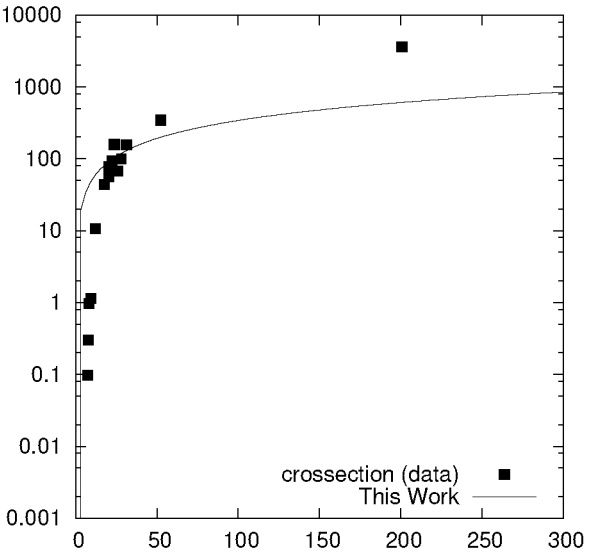

Fig. 12. Plot of the theoretical SCM prediction of cross-section of the J/Ψ inclusive production in Au + Au collision at different energies by the solid line against the experimental data.[50]

Table 1. The rapidity distribution of PP reaction at $\sqrt{s} = 200$ GeV.

	Experimental result	Calculated theoretical result
$B\dfrac{dN}{dy}\Big\|_{y=0}$ (pp)	$1.46 \pm 0.23(\text{stat}) \pm 0.22(\text{sys}) \pm 0.15(\text{abs}) \times 10^{-6}$	1.82×10^{-6}

The experimental data are taken from Ref. 50 and they are plotted in Fig. 12. The model-based theoretical curve are plotted and is shown by the solid curve in the same figure.

4.6.2. *The rapidity distribution of proton–proton reactions at* $\sqrt{s} = 200$ GeV

The J/Ψ invariant yield in the proton–proton induced reactions at $\sqrt{s} = 200$ GeV at midrapidity is calculated with the help of Eqs. (1) and (7) and the theoretical result is compared with the experimental results in Table 1. The data is taken from Ref. 48. Here B is the branching fraction $(5.93 \pm 0.10 \times 10^{-2})$ (Ref. 48) of $J/\Psi \to e^+e^-$.

4.6.3. *The average multiplicity ratio of* J/Ψ *to the negative hadrons*

In calculating the average multiplicity ratio of J/Ψ to the negatively charged hadrons, we made here a simple extrapolation of $p - p$ collisions at $\sqrt{s} = 130$ GeV from Fig. 5 and Eq. (11). The relation now becomes

$$\frac{\langle n_{J/\Psi}\rangle_{\text{Au Au}}}{\langle h^- \rangle} \times 10^6 \simeq 1.05\,. \tag{30}$$

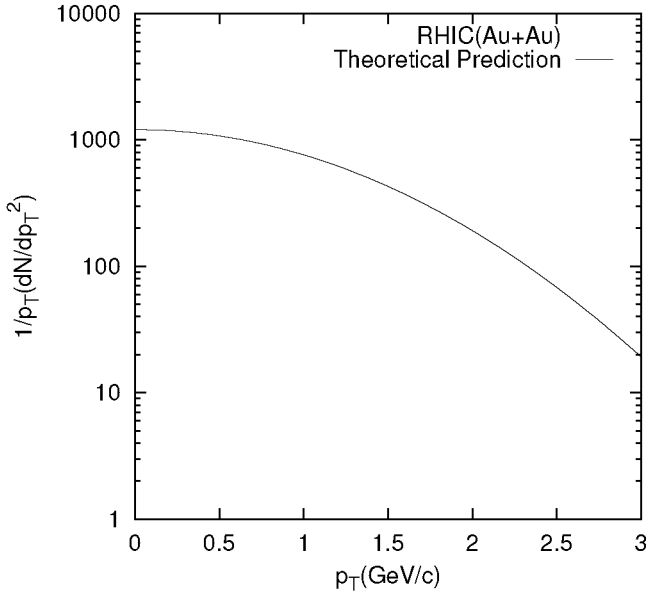

Fig. 13. Plot of the theoretical SCM prediction of p_T distribution of the J/Ψ inclusive production in Au + Au collision at RHIC at $\sqrt{s} = 130$ GeV by the solid line.

4.6.4. *The transverse momentum distribution*

The transverse momentum distribution of Au + Au collisions at $\sqrt{s} = 130$ GeV in the light of SCM will be

$$\left.\frac{1}{p_T}\frac{dN}{dp_T}\right|_{\mathrm{Au\,Au}} = 1204.24\exp(-0.46p_T^2)\,. \tag{31}$$

The predicted curve is plotted in Fig. 13. Here, we use Eq. (23) to calculate the transverse momentum distribution of Au + Au collisions at $\sqrt{s} = 130$ GeV.

4.6.5. *The average transverse momentum*

We have calculated the average transverse momentum for Au + Au collisions at $\sqrt{s} = 130$ GeV with the help of Eq. (6), and the predicted value of the $\langle p_T\rangle_{\mathrm{Au\,Au}} \sim 1.93$ GeV/c for the Au + Au collisions at $\sqrt{s} = 130$ GeV. The value of κ of that equation is taken here ~ 0.32. The predictive plot based on the model for our choice is shown by a point in Fig. 14.

5. Final Remarks

The model (SCM) we applied here is not based on any of the tenets of QGP physics. In fact, this model attempts to build up, from the very outset, a somewhat different and independent approach. Still, one observes here a modestly satisfactory description of the measured data in diverse particle–particle, particle–nucleus and

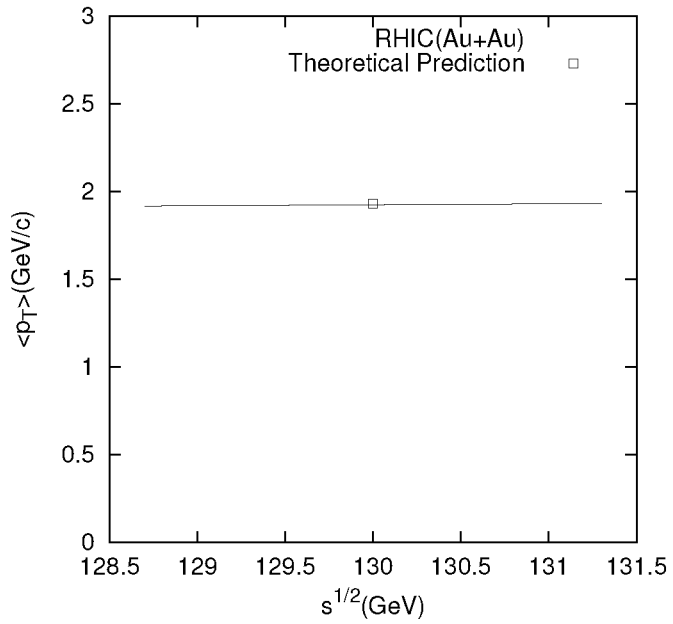

Fig. 14. Plot of theoretical SCM prediction of $\langle p_T \rangle$ in Au + Au collisions at $\sqrt{s} = 130$ GeV by the point.

nucleus–nucleus interactions at high energies. In most cases, at the root lies here the simultaneous application of the SCM for proton-mediated part of the collisions and of the standard Glauberian approach for the nucleus-involved reactions. It is difficult to attribute the various sets of nice agreements obtained between measured data and calculated results in such widely varied reactions, ranging from *ep* scattering to Pb – Pb collisions reactions at high energies, to sheer coincidence. On the contrary, in our opinion, the success achieved in the present work reflects only the efficacy of both the used models.

Obviously, the points that emerge as the natural outcome of this study are as follows:

(i) The production of J/Ψ particles is not clear, unique and unambiguous signature of QGP formation.
(ii) The production is neither suppressed nor enhanced; rather the scenario is only of usual nature, as the case is with some other hadrons like pion, kaon, etc.; though it is accepted that, according to this model, the psions (J/Ψ particles) are considered to be the bound states of a massive variety of mesons called omega mesons.[42]
(iii) The two-sector (low energy and high energy) behavior, as proposed by Gorenstein *et al.*,[4] is not supported by the present mechanism of particle and J/Ψ meson production.

(iv) The predictions made in our work for RHIC experiments involving Au + Au collisions at $\sqrt{s} = 130$ GeV offer a viable testing tool of the model applied here in the near future.

Very recently, the data-sets have started flowing in from the BNL-RHIC experiments involving Au + Au reactions at $\sqrt{s_{NN}} = 200$ GeV (Ref. 48) and also from proton–proton collisions at $\sqrt{s_{NN}} = 200$ GeV (Ref. 49). But as the measured observables are somewhat different from what they are here, we cease to treat them in the present work. We hope to present them in a future work, as the implications of these observations seem to be of much import within the context of the Standard Model, as pointed out by Chaudhuri[50] in a very recent paper.

(v) The connectors used for conversions of the results of nucleon–nucleon collisions and to those of nucleus–nucleus interactions work modestly well.

References

1. Q. H. Zhang, *Int. J. Mod. Phys.* **A17**, 109 (2002).
2. J. O. Schimitt, G. C. Nayak, H. Stöcker and W. Greiner, *Phys. Lett.* **B498**, 163 (2001).
3. T. Matsui and H. Satz, *Phys. Lett.* **B178**, 416 (1986).
4. M. I. Gorenstein, A. P. Kostyuk, H. Stöcker and W. Greiner, *Phys. Lett.* **B524**, 265 (2002).
5. S. Digal, S. Fortunato, P. Petrec and H. Satz, *Phys. Lett.* **B549**, 101 (2002).
6. C. Y. Wong, E. S. Swanson and T. Barnes, *Phys. Rev.* **C64**, 014903 (2002).
7. B. Zhang *et al.*, *Phys. Lett.* **B546**, 63 (2002).
8. B. K. Patra and D. K. Srivastava, *Phys. Lett.* **B505**, 113 (2001).
9. A. Nogová, N. Pišútová and J. Pišút, *Phys. Lett.* **B500**, 59 (2001).
10. N. Armesto and A. Capella, *J. Phys.* **G23**, 1969 (1997).
11. E672/706 Collab. (V. Abramov *et al.*), Fermilab-Pub-91/62-E.
12. NA50 Collab. (M. C. Abreu *et al.*), CERN-EP-2000-141.
13. NA50 Collab. (M. C. Abreu *et al.*), *Phys. Lett.* **B521**, 195 (2001).
14. NA50 Collab. (M. C. Abreu *et al.*), *Phys. Lett.* **B450**, 456 (1999).
15. NA50 Collab. (M. C. Abreu *et al.*), *Phys. Lett.* **B410**, 337 (1997).
16. A. G. Clark *et al.*, *Nucl. Phys.* **B142**, 29 (1978).
17. C. Kourkomelis *et al.*, *Phys. Lett.* **B91**, 481 (1980).
18. K. J. Anderson *et al.*, *Phys. Rev. Lett.* **37**, 799 (1976).
19. J. McEwen *et al.*, *Phys. Lett.* **B121**, 198 (1983).
20. J. Lebritton *et al.*, *Phys. Lett.* **B81**, 401 (1979).
21. M. Cordon *et al.*, *Phys. Lett.* **B98**, 220 (1980).
22. B. A. Kniehl and L. Zwirner, hep-ph/0112199; also at DESY 01-196 MPI-PhT/2001-29.
23. NA38 Collab. (M. C. Abreu *et al.*), in *Proc. Int. Conf. Phys. Astrophys. Quark-Gluon Plasma 1988* (Narosa, India), p. 63.
24. NA38 Collab. (M. C. Abreu *et al.*), *Phys. Lett.* **B449**, 128 (1999).
25. A. P. Kostyuk, hep-ph/0111096.
26. M. I. Gorenstein, A. P. Kostyuk, H. Stöcker and W. Greiner, *J. Phys.* **G27**, L47 (2001).
27. K. A. Bugaev, M. Gaździcki and M. I. Gorenstein, *Phys. Lett.* **B544**, 127 (2002).

28. M. Gaździcki and M. I. Gorenstein, *Phys. Rev. Lett.* **83**, 4009 (1999).
29. B. Z. Kopeliovich, A. Polleri and J. Hüfner, *Phys. Rev. Lett.* **87**, 112302 (2001).
30. J. P. Blaizot and J. Y. Ollitrault, *Phys. Rev.* **D39**, 232 (1989).
31. M. C. Abreu *et al.*, *Phys. Lett.* **B477**, 28 (2000).
32. N. Armesto *et al.*, nucl-th/0104004.
33. A. Capella, A. B. Kaidalov and D. Sousa, to appear in *Phys. Rev. C* (2002), nucl-th/0105021.
34. D. Kharzeev, in *Physics and Astrophysics of Quark Gluon Plasma*, eds. B. C. Sinha, D. K. Srivastava and Y. P. Viyogi (Narosa, India, 1998), p. 407.
35. R. C. Hwa, J. Pišút and N. Pišútová, *Phys. Rev.* **C64**, 054611 (2001).
36. G. Sanyal, Ph.D. Thesis, Calcutta University (1979).
37. S. Bhattacharyya, *J. Phys.* **G14**, 9 (1988), and references therein.
38. P. Guptaroy, S. Bhattacharyya, B. De and D. P. Bhattacharyya, *Fizika* **B10**, 103 (2001).
39. P. Guptaroy, B. De, S. Bhattacharyya and D. P. Bhattacharyya, *Heavy Ion Physics* **15**, 103 (2002).
40. P. Guptaroy, B. De, S. Bhattacharyya and D. P. Bhattacharyya, *Int. J. Mod. Phys.* **A17**, 1159 (2002).
41. P. Guptaroy, B. De, S. Bhattacharyya and D. P. Bhattacharyya, *Int. J. Mod. Phys.* **E12**, 493 (2003).
42. S. Bhattacharyya and P. Bandyopadhyay, *Lett. Nuovo Cimento* **18**, 494 (1977).
43. C. Y. Wong, *Introduction to High-Energy Heavy Ion Collisions* (World Scientific, Singapore, 1994).
44. A. Bialas, M. Bleszynki and W. Czyz, *Nucl. Phys.* **B111**, 461 (1976).
45. K. Kadija, I. Derado, N. Schmitz and P. Seyboth, *Z. Phys.* **C66**, 393 (1995).
46. S. Bhattacharyya, *Proc. 20th ICRC*, Vol. 5 (Moscow, 1987), p. 170, and references therein.
47. H. R. Schmidt and J. Schukraft, *J. Phys.* **G19**, 1705 (1993).
48. PHENIX Collab. (S. S. Adler *et al.*), nucl-ex/0305030.
49. PHENIX Collab. (S. S. Adler *et al.*), nucl-ex/0307019.
50. A. K. Chaudhuri, nucl-th/0307029.